ce/papers Proceedings in civil engineering

Ernst & Sohn A Wiley Brand

ORIGINAL ARTICLE

ibausil
F. A. Finger-Institut für Baustoffkunde
Bauhaus-Universität Weimar

Interaction of layered double hydroxide phases with chloride ions

Alisa Machner[1]

Correspondence

Prof. Dr. Alisa Machner
Technical University of Munich
TUM School of
Engineering and Design
Department for
Materials Engineering
cbm Centre for Building Materials
Professorship for Mineral
Construction Materials
Franz-Langinger-Str. 10
81245 Munich - Germany

Email: alisa.machner@tum.de

[1] Technical University of Munich, Germany

Abstract

For the sustainable transition of the construction sector, the durability of cementitious materials needs to be guaranteed. This requires a fundamental understanding of the deterioration mechanisms for example how the ingress of potentially detrimental ions affects the composition of the pore solution as well as the phase assemblage. This contribution links results from several research projects investigating the changes in layered double hydroxides (LDH) composition upon exposure to chlorides. The Cl/Al ratio in chloride-containing AFm phases depends on the chloride concentration as well as on the pH of the liquid phase. In addition, the amount of AFm phases is affected by the pH. Another member of the LDH group, hydrotalcite (Ht), can also incorporate chloride ions into the interlayer and exhibit a similar chloride-binding capacity as stoichiometric Friedel's salt. However, the chloride-binding capacity of Ht also depends on the composition of the pore solution. These findings aid the fundamental understanding of chloride-binding mechanisms of cementitious materials. This is especially important, as the pH and calcium availability in the pore solution of hydrated cement may be altered during its service life. Moreover, the results may help to accurately predict the durability performance of samples in the laboratory.

Keywords

Chloride exposure, chloride binding, AFm phases, Friedel's salt, Kuzel's salt, hydrotalcite, pH, solid solution

1 Introduction and motivation

The need of today's society to reduce greenhouse gas emission and primary resource consumption is prevailing in discussions and media more than ever. On the one hand, the construction sector is a massive contributor to these current problems. It has been estimated that cement production is responsible for 7-8 % of the total anthropogenic CO_2 emissions [1,2]. In addition, in 2018 the demand for aggregates in concrete production was 587 million tonnes, in Germany alone [3]. On the other hand, due to the large quantities of construction materials used globally each year and the predicted further growth of this demand, there exists an enormous potential to reduce emissions and resource consumption within this sector. Annually, 14 billion tonnes of cement are produced around the globe [4]. Consequently, already a reduction of only 10% CO_2 emissions per tonne cement would mean a saving of 840 million tonnes CO_2 each year. Similarly, approaches to develop the construction sector towards a circular economy can cause tremendous savings in resource consumption.

While the reduction of CO_2 emissions during the production of cementitious materials is of outmost importance, the durability of these materials also needs to be increased in order to elongate their service life and to avoid unnecessary maintenance or replacement. For this, a fundamental understanding of the deterioration mechanisms that determine the durability of construction materials is needed. With this knowledge, deterioration can either be completely avoided or at least significantly delayed. This approach therefore directly addresses the 5-step European waste hierarchy [5] of a circular economy from the most important angle: avoidance and prevention of waste.

During its service life, concrete is challenged by various deterioration mechanisms. Several of these mechanisms involve the ingress of deleterious, external ions, e.g. chlorides. The ingress of external chloride ions affects the composition of the whole system and therefore the composition of the pore solution as well as the solid hydration phase assemblage. This is especially important for hydration phases that are to a certain extent variable in their composition.

https://doi.org/10.1002/cepa.2992

The main hydration phase of Portland cement, C-S-H, is a very variable hydrate. Its Ca/Si ratio as well as water content or morphology can vary depending on the composition of the cementitious material, curing temperature and time [6–11]. In addition, C-S-H phases are known to be able to accommodate ions, such as chlorides or alkalis, in their interlayer [12] or the electric double layer at their surface [13,14].

Next to C-S-H, layered double hydroxides (LDH) are important hydration phases of Portland (composite) cements, which are also variable in composition. These layered mineral phases are known to rapidly interact with the liquid phase they are in contact with and easily change their interlayer composition [15–19].

Even though these phases have been known and investigated for a long time, it is still not ultimately possible to predict how these phases interact in variable hydrated cementitious systems [20,21]. Fundamental knowledge on the chloride binding of the hydration phases and parameters affecting it is needed to allow for improved estimation of the chloride ingress and therefore chloride resistance in concrete [21–23].

This current contribution aims to link results from various research projects investigating the changes in LDH composition in hydrated cement paste and mortar samples upon chloride exposure. First, a short literature review of the structure and formation of a selection of LDH phases (AFm and hydrotalcite) in hydrated cementitious systems is given. In a second part, the interaction of various LDH phases with chloride ions and parameters that affect this interaction are presented based on a selection of previous studies. Lastly, practical implications of these findings and further research needs are summarized within this contribution.

2 Layered double hydroxides – LDH

LDH, also referred to as anionic clays, are mineral phases that consist of positively charged main layers and negatively charged interlayers. Their crystal structure can be derived from brucite [24]. The main layer consists of metals (here abbreviated with Me), where the partial substitution of tri-valent for bi-valent metals charges this layer positively. To maintain electrical neutrality, the interlayer incorporates monovalent or divalent anions (here abbreviated with A) like OH^-, Cl^-, CO_3^{2-} or SO_4^{2-}. The general formula of LDH phases can be given as $[Me^{2+}_{1-x}\,Me^{3+}_{x}\,(OH)_2][A^{Y-}]_{x/y}\cdot nH_2O$ [25]. From this general formula, it becomes clear that the composition of LDH is rather variable. Especially the composition of the interlayer can vary considerably and easily, which makes LDH perfect materials for processes in which ion exchange mechanisms are required [26].

Overall, there exist many various LDH phases. Naturally occurring LDH are categorized within the so-called hydrotalcite supergroup [24]. From the perspective of a cement chemist, there are two groups within this supergroup that are of special interest: the hydrocalumite and the hydrotalcite group. This is because generally well-known hydration phases of Portland (composite) cements, such as the general subgroup of AFm phases and hydrotalcite-like phases belong to these two groups. In the following both subgroups of hydration phases will be described from a structural perspective as well as their formation in hydrating cementitious materials.

2.1 AFm phases

AFm phases (Alumina-ferric monophase) are Ca-Al/Fe containing representatives of LDH. Their structure is derived from hydrocalumite [27,28], which belongs to the hydrotalcite supergroup [24]. The layered structure of AFm phases consists commonly of positively charged Ca-Al main layers with a fixed cation ratio [29,30]. However, the replacement of aluminium with iron is possible in the AFm structure [31–35]. To maintain charge balance, their structure also consists of negatively charged interlayers. Their general formular can be described as $[Ca_2(Al,Fe)(OH)_6]\cdot X\cdot nH_2O$ [28,36].

Depending on the composition of the interlayer, various types of AFm phases can be differentiated. Hydroxy-AFm is an unstable AFm phase, that is often replaced by other AFm phases in the hydration phase assemblage of cement [28,37]. In the case where sulphate is present in the interlayer, the resulting phase is called monosulphate (also called kuzelite, with the formula $Ca_4Al_2(OH)_{12}(SO_4)\cdot 6H_2O$). Though it should be noted that various hydration stages are known for monosulphate depending on the relative humidity [38]. An illustration of the crystal structure of kuzelite is given in Figure 1.

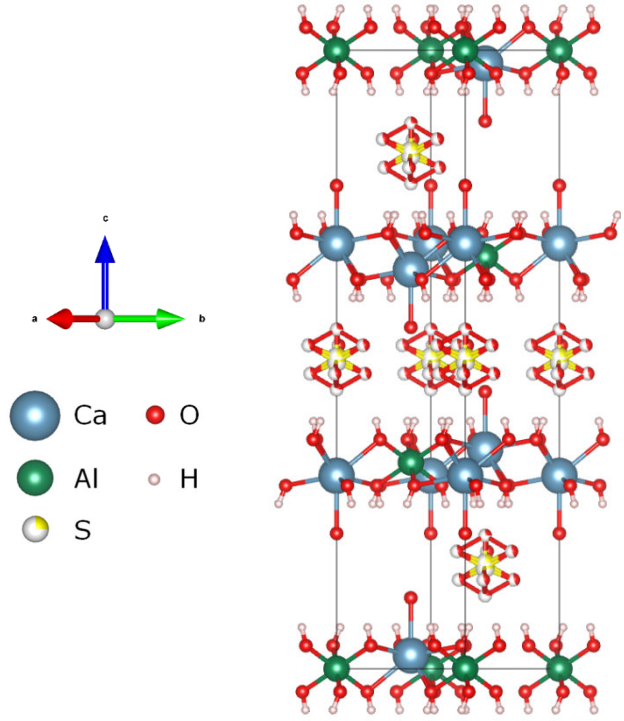

Figure 1 Illustration of kuzelite crystal structure. Structural data from [30], illustration by VESTA [39]

Already at small amounts of carbonate present in the cementitious system, other AFm phases such as hemicarbonate ($Ca_4Al_2(CO_3)0.5(OH)_{13}\cdot 5.5H_2O$) and monocarbonate ($Ca_4Al_2(CO_3)(OH)_{12}\cdot 5H_2O$) are known to form during hydration of Portland cement [28,40–43].

Especially composite cements containing a combination of Al-rich SCMs and carbonates (e.g. limestone or dolomite)

are known to form considerable amounts of the carbonate-containing AFm phases during their hydration [44–49].

In the presence of chloride ions, e.g. due to exposure to de-icing salts or sea water, chloride-containing AFm phases, such as Friedel's salt (short: Fs, formula: $(3CaO{\cdot}Al_2O_3{\cdot}CaCl_2{\cdot}10H_2O)$ or Kuzel's salt (short: Ku, formula: $3CaO{\cdot}Al_2O_3{\cdot}0.5CaSO_4{\cdot}0.5CaCl_2{\cdot}11H_2O$) are known to form. However, the composition of Friedel's salt is not fixed stoichiometrically and factors impacting the Cl/Al ratio of the AFm phases are discussed in section 3.1.

2.2 Hydrotalcite-like phases

Hydrotalcite is the name giving mineral for a group and supergroup within the LDH nomenclature [24], as it was the first LDH to be discovered [50]. Hydrotalcite as a mineral name refers to an LDH with a main layer consisting of magnesium and aluminium and the formula $[Mg_6Al_2(OH)_{16}](CO_3){\cdot}4H_2O$ [51].

As typical for LDH members, the composition of the interlayer of hydrotalcite is variable. Hence, it shows excellent ion exchange properties [15–19]. For cementitious materials, mostly anions such as OH^-, CO_3^{2-}, and Cl^- are of interest for the interlayer composition of hydrotalcite. In contrast to AFm phases, the cation ratio in the main layer is not fixed in hydrotalcite-like minerals. While the natural mineral shows a Mg/Al ratio of 3, also lower Mg/Al ratios of approx. 2 are commonly reported in cementitious systems [11,52–56]. Hence, various hydrotalcite-like phases, e.g. meixnerite $(Mg_6Al_2(OH)_{18}{\cdot}4(H_2O))$ with a Mg/Al ratio of 3 as an example for the hydroxy version, or quintinite $(Mg_4Al_2(OH)_{12}(CO_3){\cdot}3H_2O)$ as an example of a phase with a Mg/Al ratio of 2, exist [57,58]. Figure 2 shows an illustration of the crystal structure of a hydrotalcite-like phase. Commonly hydrotalcite-like phases are referred to by simply "hydrotalcite" (short: Ht) as well, as done in this present study.

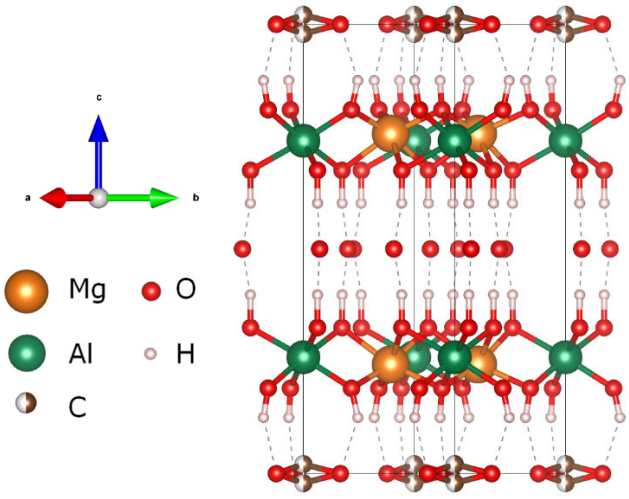

Figure 2 Illustration of quintinite crystal structure as an example of hydrotalcite-like phases. Structural data from [58], illustration by VESTA [39]

As hydrotalcite requires a sufficient amount of magnesium and aluminium to form, it is commonly observed to form in hydrating cements that contain ground granulated blast furnace slag (GGBFS) [11,53,54,59] or in GGBFS-containing alkali-activated materials [19], all of which typically contain reactive magnesium. In addition, its formation was reported in hydrating cements that contain dolomite [52,60] or a combination of dolomite and small amounts of metakaolin [49,61,62].

Like AFm phases, Ht can accommodate chloride ions in its interlayer depending on various factors as discussed in chapter 3.2.

3 Interaction of LDH with chloride ions

In the following, the interaction of LDH phases with chloride ions will be discussed in detail. In general, the chloride binding by LDH is due to their ability to incorporate a variety of anions into their interlayer. However, there are several parameters that affect this interaction. These parameters are discussed for chloride-containing AFm phases (Cl-AFm) and chloride-containing hydrotalcite (Cl-Ht) in the following based on the selection of previous studies.

3.1 Chloride binding of AFm phases

AFm phases formed during the hydration of (composite) cements are able to incorporate chloride into their interlayer. The two main chloride-containing AFm phases are Friedel's salt and Kuzel's salt. However, it is important to note that the composition of Friedel's salt is not fixed stoichiometrically as there exists a solid solution (Fs_{ss}) between Fs and monocarbonate, hemicarbonate or hydroxy AFm [42,63–69]. For Kuzel's salt only limited solid solutions with either monosulphate or Friedel's salt have been reported [63,66]. In addition, Kuzel's salt has been observed to be unstable in the presence of even small amounts of carbonate [63].

The Cl/Al ratio in Fs_{ss} depends on the chloride concentration of the solution the solids are in contact with [63]. With increasing Cl concentration of the exposure and thereby pore solution, the Cl/Al ratio of Fs_{ss} was shown to increase [63]. This change in Cl/Al ratio has recently also been incorporated into the thermodynamic database "cemdata18" by Lothenbach et al. [70], which allows the prediction of the Cl/Al ratio of Fs_{ss} depending on the chloride concentration of the liquid phase.

In addition to the Cl concentration, the amount of chlorides bound by hydration phases also depends on the pH of the liquid phase. $CaCl_2$ exposure of hydrated alite or cement pastes showed an effect of pH on the chloride binding of cement pastes [71–76]. Decreasing pH enhances the physical binding of chlorides by C-S-H [71,77–79]. However, also the AFm phases contribute to the increased chloride binding at lower pH [63,79,80]. By exposing well-hydrated Portland cement pastes to chloride solutions of various pH, Hemstad et al. [80] could show that decreasing the pH of the exposure solution from approx. 13.5 to approx. 12 caused a more than double as high chloride-binding of the cement paste. By SEM-EDS point analyses of the exposed samples, it was shown that, with decreasing pH, the Cl/Al ratio in the AFm phases increased from approx. 0.4 to the 1.0, indicating the stochiometric composition of Friedel's salt at low pH [80]. In addition to the increase in the Cl/Al ratio, an overall increase in the amount of Fs_{ss} was reported upon decreasing pH [80].

Also when comparing various hydrated composite cements, the contribution of AFm phases to the overall chloride binding capacity of the cement paste is due to changes in composition as well as the amount of AFm phases change with changing composition of the cementitious system [20,69].

The results reported in [20,80] were obtained on bulk experiments with well-hydrated cement pastes. In addition to these studies, the effect of the pH on chloride binding has also been shown in diffusion experiments on mortar samples [81,82]. This was investigated by exposing mortar samples to unidirectional diffusion of solutions with the same chloride concentration but different pH. For this, a 3 % NaCl solution was used and compared to a solution were KOH was added in order to reach a high pH (approx. pH 13.2) [81,82]. Two different composite cements were used, a CEM II/C-M (S-LL) [82] and a CEM VI (S-V) [81], of which the hydration phase assemblage in the samples prepared with the CEM VI were investigated in depth after exposure. The composition of the hydration phases was investigated by SEM-EDS after exposure for 180 days to either of the exposure solutions (Figure 3).

Originally, monosulphate was the predominant AFm phase in the hydrated CEM VI samples prior to chloride exposure [81]. Depending on the pH of the exposure solution, the maximum Cl/Al ratio of the AFm phases in the samples differed. In case of NaCl exposure, Friedel's salt (Cl/Al ratio 1.0) was observed (see Figure 3 a), whereas in the case of exposure to NaCl+KOH, Kuzel's salt (Cl/Al ratio 0.5) was present (see Figure 3 b). It is known, that sulphate ions in the interlayer of monosulphate can be replaced with chloride ions [63,83]. However, compared to monocarbonate, no solid solution exists between monosulphate and Friedel's salt [63,66]. Instead of a complete solid solution, a distinct phase, Kuzel's salt, can form at lower Cl concentrations [63,83].

However, both samples have been exposed to solutions with the same chloride concentration. Consequently, any differences in the chloride concentration of the pore solution at a certain depth from the exposed surface are due to changes in the chloride ingress. In addition, the hydroxyl (OH^-) concentration in the exposure solution may also play an important role in determining the type of AFm phase formed. A solid solution between Friedel's salt and hydroxy-AFm [63] has been reported. Consequently, the formation of hydroxy-AFm might be favoured over the formation of Friedel's salt in case of NaCl+KOH exposure due to the higher hydroxyl (OH^-) concentrations than in the NaCl solution. As the hydroxyl ions compete with the chloride ions for their position in the AFm structure [63], this would also explain the lower Cl/Al ratios of the AFm phase in case of NaCl+KOH exposure compared to NaCl as shown in Figure 3 [81], which are in some cases even lower than the Cl/Al ratio in Kuzel's salt.

Besides the increase in the Cl/Al ratio, also the increase in their amount present in the samples upon a slight reduction of the pH reported on bulk cement paste samples [80] could also be verified on mortar samples [81]. Figure 4 shows the DTG curves of samples exposed to NaCl or NaCl+KOH from various depths from the exposed surface (1 - 25 mm). Towards the exposed surface, the AFm weight loss peaks shift towards lower temperatures and show a double peak for both exposures. This indicates the formation of Cl-AFm or Cl-Ht phases, as the single peak (e.g. at 25 mm) has been associated with carbonate or sulphate AFm phases [84], while the double peak has been related to the decomposition of chloride-containing AFm phases [19,80,84–86].

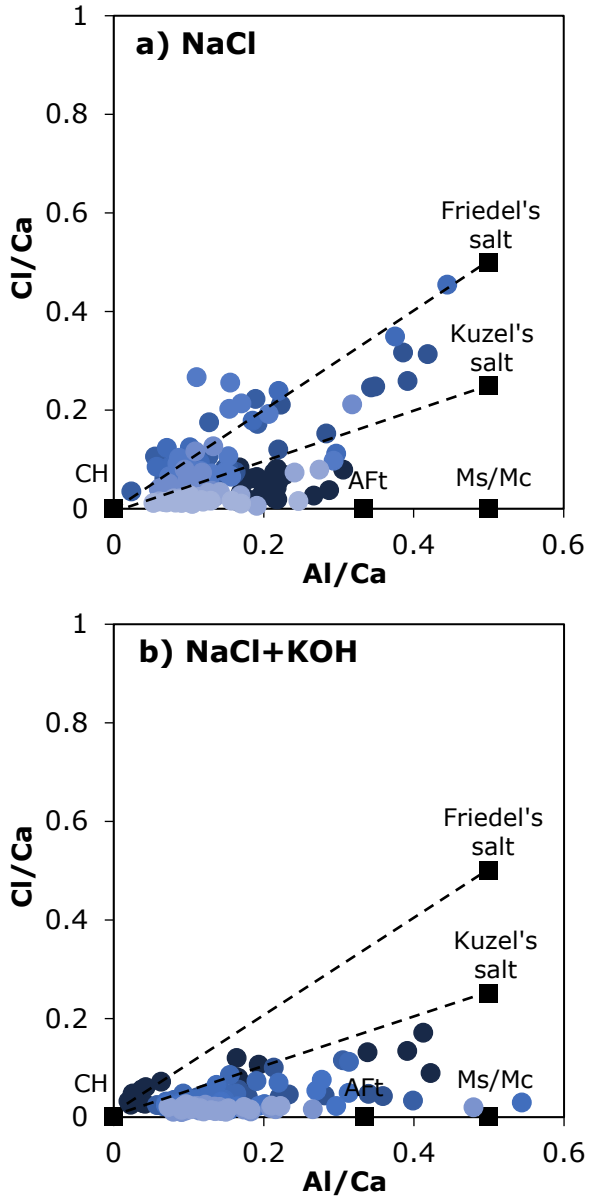

Figure 3 Cl/Ca ratio over the Al/Ca ratio of point analyses of the matrix in mortar samples exposed to a 3% NaCl (a) or 3% NaCl+KOH solution for 180 days. The depth from the exposed surface (0.03–20 mm) is indicated by colour (dark blue: 0.03 mm, light blue: 20 mm). Black squares indicate the ideal compositions of portlandite (CH), Friedel's salt, Kuzel's salt, monosulphate (Ms), monocarbonate (Mc), and ettringite (AFt). Data from [81]

As expected, the AFm weight loss peaks increase towards the exposed surface for both specimens. However, there are differences in the maximum level of the weight loss depending on the exposure solution. In the case of NaCl exposure, a considerably higher maximum AFm weight loss peak can be observed compared to samples exposed to NaCl+KOH. However, such an increase is not predicted by the thermodynamic model in that study (see [81]) as the overall aluminium content of the sample is not affected by leaching. The overall aluminium availably directly affects the chloride binding capacity of the hydrated cement

[85,87]. As reported by Baba Ahmadi et al. [20], aluminium can potentially be released from C-A-S-H phases present in hydrated cement paste upon decreasing pH, enabling the formation of additional AFm phases.

Overall, there are several parameters that affect the Cl/Al as well as the amount of Cl-AFm. Hence, the chloride binding of hydrated cement pastes is affected considerably by these parameters. Implications for practical applications and laboratory performance testing of these rather fundamental results are given in chapter 4.

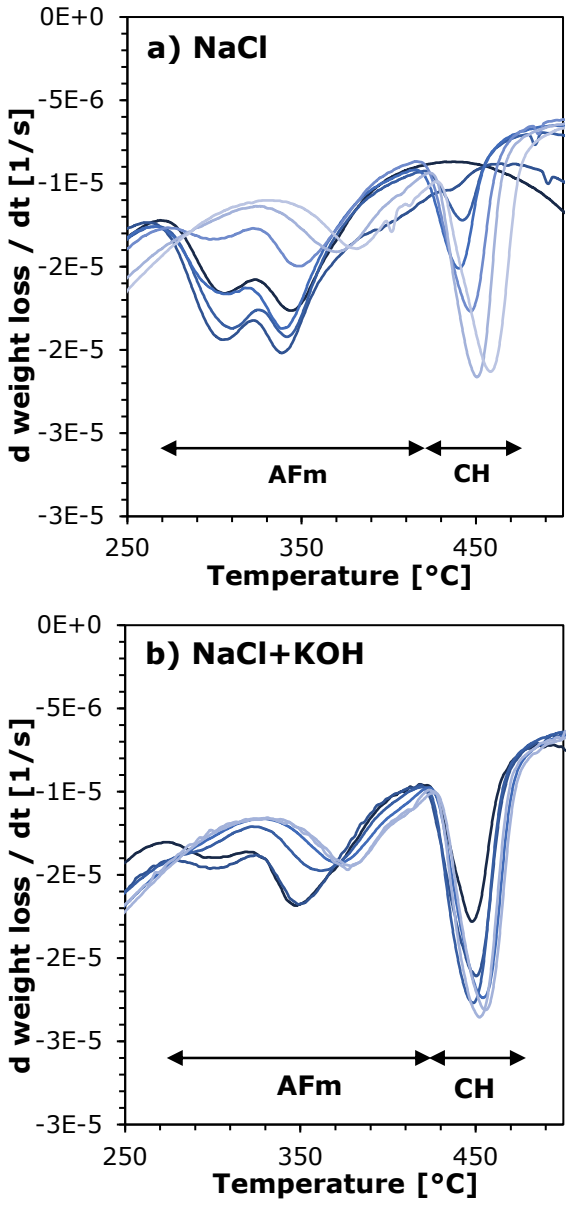

Figure 4 DTG curves of sections at various depths below the exposed surface for mortar samples exposed to a 3% NaCl (a) or 3% NaCl+KOH solution for 180 days. DTG curves are shown in the temperature range of AFm and portlandite (CH) decomposition (250–500 ◦C). The depth from the exposed surface (1 - 25 mm) is indicated by colour (dark blue: 1 mm, light blue: 25 mm). Data from [81]

3.2 Chloride binding of hydrotalcite

Hydrotalcite is known to show excellent ion exchange properties, and consequently also high chloride binding potential [15–19].

The formation of chloride-containing hydrotalcite was reported in [62,86] for composite cements containing dolomite or a combination of dolomite and metakaolin exposed to chloride solutions (NaCl or $CaCl_2$) of various concentrations. The presence of Cl-Ht was identified from its chemical composition determined with SEM-EDS and the uptake of chlorides in the interlayer by changes in the peak positions in TGA and XRD [62,86]. Figure 5 shows the diffractogram of hydrated paste samples containing 60 wt.% OPC and 40 wt.% dolomite (60C40D) that were exposed to either deionized water ($60C40D_{H2O}$) or 2 mol/L sodium chloride solution ($60C40D_{NaCl}$). The shift of the XRD peak of hydrotalcite to lower °2θ in the presence of chlorides is clearly visible when comparing the two samples. For comparison, also the peak position of Friedel's salt is indicated. The shift in the XRD peak position and in the TGA curves of Cl-Ht compared to chloride-free Ht has been previously reported by Ke et al. [19] for synthetic Ht samples. In the XRD diffractogram, a shift to lower °2θ of this peak is caused by an increase in the c-parameter [88]. This shows the incorporation of chloride into the interlayer of hydrotalcite, because chloride ions have a larger ionic radius than hydroxide ions [17–19,89].

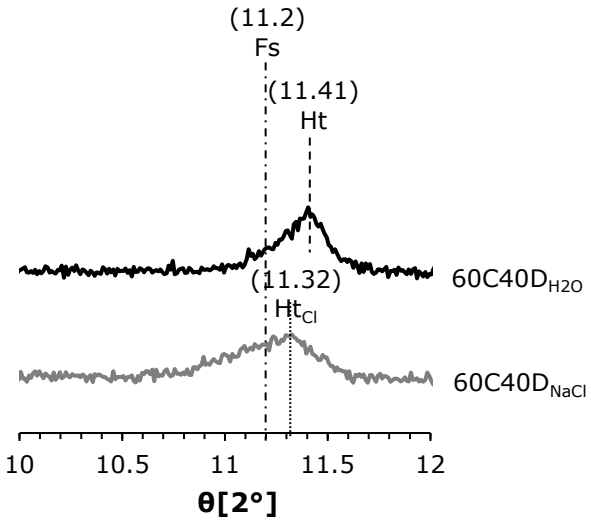

Figure 5 XRD patterns (zoomed in to the region 10-12 °2θ) of hydrated paste samples containing 40 wt.% dolomite, which were exposed to 2 mol/L NaCl solution ($60C40D_{NaCl}$) and a reference sample exposed to deionized water ($60C40D_{H2O}$). Data from [62,86]

The composition of the hydrotalcite interlayer depends on several factors. One of them is the chemical composition of the system. Divalent ions, like CO_3^{2-}, are more easily incorporated into the hydrotalcite interlayer than monovalent ions, like Cl^- [15,17,18]. Hence, the presence of carbonate ions or an increase of their amount in the system reduces the chloride-binding capacity of hydrotalcite [15,19]. However, even if carbonates are present in rather high amounts, hydrotalcite is able to contribute considerably to the chloride binding of the samples [86].

The chloride content in hydrotalcite increased when hydrated pastes are exposed to $CaCl_2$ compared to NaCl [86]. This can be shown e.g. by SEM-EDS point analyses, determining the Cl/Al ratio in the hydrotalcite as demonstrated in Figure 6. The reason for this increase in chloride binding in the case of $CaCl_2$ exposure is because the carbonate activity in the system depends on the chemical en-

vironment. When exposed to $CaCl_2$ the carbonate ion activity in the liquid phase of the samples is reduced compared to exposure to NaCl as shown in [86] by a simple thermodynamic modelling approach. A reduction in the carbonate ion activity is assumed to favour the uptake of chlorides over carbonates in the interlayer of hydrotalcite, explaining the higher chloride binding by hydrotalcite in case of $CaCl_2$ exposure.

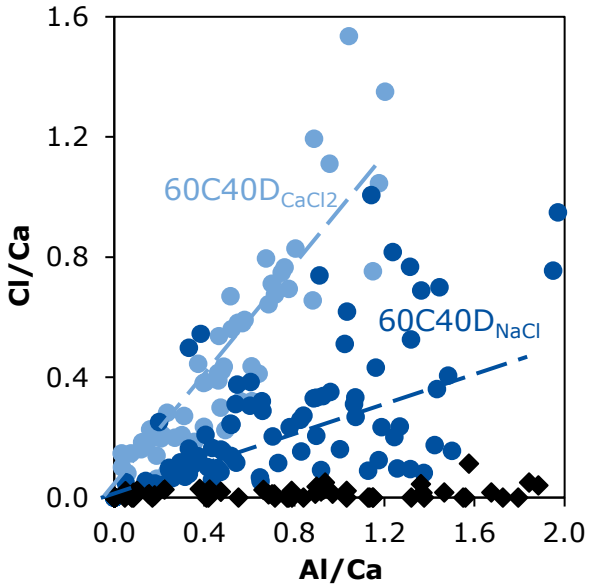

Figure 6 Cl/Ca ratio over the Al/Ca ratio of the point analyses of the reaction rims around the dolomite grains in well-hydrated paste samples containing 40 wt.% dolomite (60C40D), which were cured at 60 °C and exposed to 2 mol/L chloride solutions (NaCl or $CaCl_2$) [86]. Black diamonds represent the results for the point analyses of not-exposed samples [61]

For the members of the hydrotalcite group, not only the composition of the interlayer but also, though to a smaller extent, the Mg/Al ratio of the main layer is variable [11,52–56]. The Mg/Al ratio of the main layer depends on the amount and availability of Mg and Al in the system [11,54]. Machner et al. showed that with increasing aluminium (metakaolin) content of the system, the Mg/Al ratio of the hydrotalcite decreased in well-hydrated pastes [62,86]. The Mg/Al ratio affects the overall charge of the main layer. Since the negative charge of the interlayer is adapted to balance the positive charge of the main layer, more chlorides are reported to be incorporated in the interlayer of hydrotalcite with a lower Mg/Al ratio [17]. For hydrated dolomite and metakaolin containing composite cement pastes, this correlation between Mg/Al ratio in the main layer and chloride content in the interlayer could not be confirmed [86]. A potential explanation could be the fact that chlorides are not only incorporated in the interlayer of hydrotalcite but can also be adsorbed on their surface as shortly discussed in chapter 4.

Similarly, as described for Cl-AFm (see chapter 3.1), the chloride binding of hydrotalcite is affected by several factors. The various implications of this for concrete produced with Mg- and Al-rich SCMs are described in the following chapter.

4 Implications for practical applications and further research

The results summarized so far aid the fundamental understanding of chloride-binding mechanisms of LDH phases during chloride exposure of cementitious materials. This knowledge allows to improve predition of chloride ingress and therefore chloride resistance in concrete [15,16]. Based on results from concrete containing fly ash that was exposed to sea water for 16 years [90], De Weerdt et al. [23] showed that the majority of the total chloride content in a concrete is actually bound by solids (AFm or C-S-H). The amount of bound chlorides considerably depends on the chloride binding, and therefore the composition, of the LDH phases.

Friedel's salt is known to contribute significantly to the chloride binding capacity of hydrated cementitious materials. Similarly, hydrotalcite was shown to be able to bind considerable amounts of chloride. In order to estimate the contribution of hydrotalcite to the overall chloride binding capacity of the cement paste, not only its composition as amount of chloride per mol or per g, but also the amount of hydrotalcite formed in the sample needs to be taken into account, as done in the simplified mass balance calculation reported in [86]. Figure 7 shows the distribution of bound chlorides in C-S-H, Friedel's salt and hydrotalcite in well hydrated paste samples containing 40 wt.% dolomite or limestone exposed to 2 mol/L chloride solution (NaCl or $CaCl_2$). The comparison to the limestone-containing sample allows the classification of the impact of hydrotalcite on the chloride binding of the overall paste. Though it should be noted, that a direct quantitative comparison is not possible nor intended as the samples have been cured at different temperatures (60C40D: 60°C, 60C40L: 38 °C).

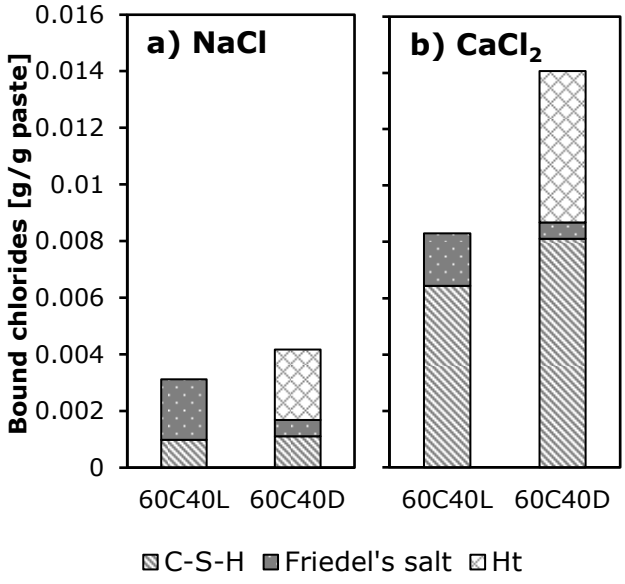

Figure 7 Amount of chlorides bound in C–S–H, Friedel's salt, and hydrotalcite calculated for well-hydrated paste samples that contain 40 wt.% of dolomite (60C40D) cured at 60°C and corresponding reference samples containing 40 wt.% limestone (60C40L) cured at 38 °C exposed to a 2 mol/L chloride solution (NaCl or $CaCl_2$). Data from [86]

Nevertheless, the estimations in Figure 7 show that hydrotalcite formed by the reaction of dolomite in composite cements, can contribute to the chloride binding of the cement paste to an extent similar to the Friedel's salt formed in equivalent samples containing limestone [86]. In cementitious systems containing slag, hydrotalcite has been predicted to bind even more chlorides than Friedel's salt [91].

It should also be noted that chlorides are not just incorporated into the interlayer of LDH but are also reported to adsorb on their surface due to the formation of an electric double layer [19,91]. To which extent chlorides are bound in the interlayer of LDH or adsorbed on their surface could not be quantified with the experimental set-up of the papers discussed here. Several insights into the interaction of LDH and chlorides are potentially also valid for other charged compounds.

Another important aspect not finally concluded on is the stability of chloride-containing LDH. These phases should be investigated with regard to their ability to retain the chlorides in their crystal structure upon various attacks on the concrete during its service life, e.g. during leaching or carbonation. This is especially important, as the pH and ion availability in the pore solution are different for different types of cement. In addition, these characteristics of hydrated cement may be altered during its service life resulting in a change in the chloride binding-capacity of the hydrated cement paste.

The results summarized in the present contribution also have an implication for chloride ingress resistance testing in the laboratory [81,82]. The leaching conditions in the laboratory set-ups are commonly drastically reduced compared to e.g. exposure to the sea, which represents an unlimited reservoir of leachate. Hence, a sample that showed reasonably good resistance to chloride ingress in the lab, can potentially perform much poorer once it is placed out in the sea. As a first step, procedures for laboratory testing that mimic realistic scenarios should be preferred, e.g. sufficiently high ratios between the volume of the exposure solution and the exposed surface, and routines for regularly replacing the exposure solution.

5 Conclusions

Chloride binding considerably affects the chloride transport and thereby the chloride ingress resistance of cementitious materials, e.g. concrete. Fundamental knowledge on chloride binding can aid the sustainable transformation of the construction sector, as it helps understanding and limiting chloride ingress in concrete.

Within this contribution, selected parameters affecting the chloride binding by various LDH phases (AFm and hydrotalcite) were discussed based on various previous research projects.

The Cl/Al ratio in Cl-AFm, depends not only on the chloride concentration but also on the pH of the liquid phase. With increasing chloride concentration and decreasing pH (down to approx. pH 12), the Cl/Al ratio of AFm was shown to increase. These observations on bulk analyses of cement pastes could be confirmed also in mortar samples exposed to unidirectional chloride diffusion. However, as not only the composition but also the amount of AFm phases changes with changing pH, it is not straightforward to determine the total contribution of each effect to the overall chloride binding capacity of the system.

Similarly, hydrotalcite (Ht) is also able to incorporate chloride ions into the interlayer and may exert a similar chloride-binding capacity as stoichiometric Friedel's salt (Fs). However, the chloride-binding capacity of hydrotalcite depends on the activity of carbonate ions in the pore solution determined by the calcium concentration.

These findings aid the fundamental understanding of chloride-binding mechanisms during chloride exposure of cementitious materials. This is especially important, as the pH and calcium availability in the pore solution of hydrated cement may be altered during its service life. In addition, these results help in identifying important parameters and conditions in laboratory performance tests, with the goal to depict the reality of deterioration mechanisms and predict the durability performance of concrete in field as reliably as possible.

6 Acknowledgements

This contribution represents a review of various studies from literature as well as own studies within previous research projects (Industrial PhD project of the Norwegian Research Council DOLCEM, project No. 241637, and European Union's Horizon 2020 research and innovation project EnDurCrete, grant agreement No. 760639). Hence, the data shown here was collected over several years in collaboration with various colleagues. I would like to thank Klaartje De Weerdt, Petter Hemstad, Arezou Baba Ahmadi, Wolfgang Kunther, as well as all project partners of the DOLCEM and EnDurCrete projects for the fruitful collaborations. In addition, I would like to thank Barbra Lothenbach, Gilles Plusquellec and Tone Østnor helpful discussions. Additional thanks go to student assistants and laboratory staff at NTNU and Sintef for their help with sample preparation and various measurements.

References

[1] Editorial (2021) *Concrete needs to lose its colossal carbon footprint.* Nature 597, Nr. 7878, pp. 593–594. https://doi.org/10.1038/d41586-021-02612-5

[2] The Cement Sustainability Initiative (2012) *Guidelines for Emissions Monitoring and Reporting in the Cement Industry*. 2. Aufl.

[3] Kreislaufwirtschaft Bau (2021) *Mineralische Bauabfälle Monitoring 2018 – Bericht zum Aufkommen und zum Verbleib mineralischer Bauabfälle im Jahr 2018*. https://kreislaufwirtschaft-bau.de.

[4] Global Cement and Concrete Association, *Cement and concrete around the world*. https://gccassociation.org/concretefuture/cement-concrete-around-the-world/.

[5] European Parliament and Council (2008) *EU-Directive 2008/98/EC, L 312/3.*

[6] Gallucci, E.; Zhang, X.; Scrivener, K. L. (2013) *Effect of temperature on the microstructure of calcium silicate hydrate (C-S-H)*. Cement and Concrete Research 53, S. 185–195. https://doi.org/10.1016/j.cemconres.2013.06.008

[7] Rossen, J. E.; Lothenbach, B.; Scrivener, K. L. (2015) *Composition of C–S–H in pastes with increasing levels of silica fume addition*. Cement and Concrete Research 75, S. 14–22. https://doi.org/10.1016/j.cemconres.2015.04.016

[8] Love, C. A.; Richardson, I. G.; Brough, A. R. (2007) *Composition and structure of C–S–H in white Portland cement–20% metakaolin pastes hydrated at 25 °C.* Cement and Concrete Research 37, H. 2, S. 109–117. https://doi.org/10.1016/j.cemconres.2006.11.012

[9] Richardson, I. G. (1999) *The nature of C-S-H in hardened cements.* Cement and Concrete Research 29, H. 8, S. 1131–1147. https://doi.org/10.1016/S0008-8846(99)00168-4

[10] Girão, A. V. et al. (2010) *Composition, morphology and nanostructure of C–S–H in 70% white Portland cement–30% fly ash blends hydrated at 55°C*. Cement and Concrete Research 40, H. 9, S. 1350–1359. https://doi.org/10.1016/j.cemconres.2010.03.012

[11] Taylor, R.; Richardson, I. G.; Brydson, R.M.D. (2010) *Composition and microstructure of 20-year-old ordinary Portland cement–ground granulated blast-furnace slag blends containing 0 to 100% slag*. Cement and Concrete Research 40, H. 7, S. 971–983. https://doi.org/10.1016/j.cemconres.2010.02.012

[12] L'Hôpital, E. et al. (2016) *Alkali uptake in calcium alumina silicate hydrate (C-A-S-H).* Cement and Concrete Research 85, S. 122–136. https://doi.org/10.1016/j.cemconres.2016.03.009

[13] Labbez, C. et al. (2007) *Experimental and theoretical evidence of overcharging of calcium silicate hydrate.* Journal of Colloid and Interface Science 309, Nr. 2, pp. 303–307. https://doi.org/10.1016/j.jcis.2007.02.048

[14] Plusquellec, G.; Nonat, A. (2016) *Interactions between calcium silicate hydrate (C-S-H) and calcium chloride, bromide and nitrate*. Cement and Concrete Research 90, S. 89–96. https://doi.org/10.1016/j.cemconres.2016.08.002

[15] Châtelet, L. et al. (1996) *Competition between monovalent and divalent anions for calcined and uncalcined hydrotalcite: anion exchange and adsorption sites*. Colloids and Surfaces A 111, H. 3, S. 167–175.

[16] Kayali, O.; Khan, M. S. H.; Sharfuddin Ahmed, M. (2012) *The role of hydrotalcite in chloride binding and corrosion protection in concretes with ground granulated blast furnace slag*. Cement and Concrete Composites 34, H. 8, S. 936–945. https://doi.org/10.1016/j.cemconcomp.2012.04.009

[17] Miyata, S. (1975) *The Syntheses of Hydrotalcite-Like Compounds and Their Structures and Physico-Chemical Properties I – The Systems Mg^{2+}-Al^{3+}-NO_3^-, Mg^{2+}-Al^{3+}-Cl^-, Mg^{2+}-Al^{3+}-ClO_4^-, Ni^{2+}-Al^{3+}-Cl^- and Zn^{2+}-Al^{3+}-Cl^-*. Clays and Clay Minerals 23, H. 5, S. 369–375. https://doi.org/10.1346/CCMN.1975.0230508

[18] Miyata, S. (1983) *Anion-Exchange Properties of Hydrotalcite-Like Compounds*. Clays and Clay Minerals 31, H. 4, S. 305–311. https://doi.org/10.1346/CCMN.1983.0310409

[19] Ke, X.; Bernal, S. A.; Provis, J. L. (2017) *Uptake of chloride and carbonate by Mg-Al and Ca-Al layered double hydroxides in simulated pore solutions of alkali-activated slag cement*. Cement and Concrete Research 100, S. 1–13. https://doi.org/10.1016/j.cemconres.2017.05.015

[20] Babaahmadi, A. et al. (2022*) Chloride binding in Portland composite cements containing metakaolin and silica fume*. Cement and Concrete Research 161, S. 106924. https://doi.org/10.1016/j.cemconres.2022.106924

[21] De Weerdt, K. (2021) *Chloride binding in concrete: recent investigations and recognised knowledge gaps: RILEM Robert L'Hermite Medal Paper 2021*. Materials and Structures 54, H. 6. https://doi.org/10.1617/s11527-021-01793-9

[22] Martín-Pérez, B. et al. (2000) *A study of the effect of chloride binding on service life predictions.* Cement and Concrete Research 30, H. 8, S. 1215–1223. https://doi.org/10.1016/S0008-8846(00)00339-2

[23] De Weerdt, K. et al. (2023) *Chloride profiles – What do they tell us and how should they be used?* Cement and Concrete Research submitted for special issue for 16th International Congress on the Chemistry of Cement 2023.

[24] Mills, S. J. et al. (2012) *Nomenclature of the hydrotalcite supergroup - Natural layered double hydroxides*. Mineralogical Magazine 76, H. 5, S. 1289–1336. https://doi.org/10.1180/minmag.2012.076.5.10

[25] Evans, D. G.; Slade, R. C. T. (2006) *Structural Aspects of Layered Double Hydroxides*. Duan, X.; Evans, D. G. [Hrsg.] Layered Double Hydroxides. Berlin, Heidelberg: Springer Berlin Heidelberg, S. 1–87.

[26] Wang, Q.; O'Hare, D. (2012) *Recent advances in the synthesis and application of layered double hydroxide (LDH) nanosheets*. Chemical reviews 112, Nr. 7, pp. 4124–4155. https://doi.org/10.1021/cr200434v

[27] Buttler, F. G.; Dent Glasser, L. S.; Taylor, H. F. W. (1959) *Studies on $4CaO{\cdot}Al_2O_3{\cdot}13H_2O$ and the Related Natural Mineral Hydrocalumite.* Journal of the

American Ceramic Society 42, H. 3, S. 121–126. https://doi.org/10.1111/j.1151-2916.1959.tb14078.x

[28] Matschei, T.; Lothenbach, B.; Glasser, F. P. (2007) *The AFm phase in Portland cement.* Cement and Concrete Research 37, H. 2, S. 118–130. https://doi.org/10.1016/j.cemconres.2006.10.010

[29] Allmann, R. (1968) *Die Doppelschichtstruktur der plaettchenfoermigen Calcium-Aluminium-Hydroxysalze am Beispiel des $3CaO{\cdot}Al_2O_3{\cdot}CaSO_4{\cdot}12H_2O$.* Neues Jahrbuch für Mineralogie (Monatshefte), S. 140–144.

[30] Allmann, R. (1977) *Refinement of the hybrid layer structure $[Ca_2Al(OH)_6]^+{\cdot}[1/2SO_4{\cdot}3H_2O]^-$*. Neues Jahrbuch für Mineralogie (Monatshefte), S. 136–144.

[31] Dilnesa, B. Z. et al. (2011) *Iron in carbonate containing AFm phases*. Cement and Concrete Research 41, H. 3, S. 311–323. https://doi.org/10.1016/j.cemconres.2010.11.017

[32] Dilnesa, B. Z. et al. (2012) *Stability of Monosulfate in the Presence of Iron.* Journal of the American Ceramic Society 95, H. 10, S. 3305–3316. https://doi.org/10.1111/j.1551-2916.2012.05335.x

[33] Dilnesa, B. Z. et al. (2014) *Fe-containing phases in hydrated cements*. Cement and Concrete Research 58, S. 45–55. https://doi.org/10.1016/j.cemconres.2013.12.012

[34] Kuzel, H.-J. (1968) *Ersatz von Al^{3+} durch Cr^{3+} und Fe^{3+} in $3CaO{\cdot}Al_2O_3{\cdot}CaCl_2{\cdot}nH_2O$ und $2CaO{\cdot}Al_2O_3{\cdot}CaSO_4{\cdot}nH_2O$*. Zement Kalk Gips 21, H. 12, S. 493–499.

[35] Ecker, M. (1998) *Diadochiebeziehungen in Calciumaluminatferraten und deren Hydratationsprodukten* [PhD Thesis]. Martin-Luther-Universität Halle-Wittenberg. Hellesches Jahrbuch für Geowissenschaften, Reihe B.

[36] François, M.; Renaudin, G.; Evrard, O. (1998) *A Cementitious Compound with Composition $3CaO{\cdot}Al_2O_3{\cdot}CaCO_3{\cdot}11H_2O$*. Acta Crystallographica Section C Crystal Structure Communications 54, H. 9, S. 1214–1217. https://doi.org/10.1107/S0108270198004223

[37] Wells, L. S.; Clarke, W. F.; McMurdie, H. F. (1943) *Study of the system $CaO{\sim}Al_2O_3{\sim}H_2O$ at temperatures of 21° and 90° C*. Journal of Research of the National Bureau of Standards 30, S. 367–409.

[38] Pöllmann, H. (2007) *Characterization of Different Water Contents of Ettringite and Kuzelite.* Proceedings of the 12th International Congress on the Chemistry of Cement. Montreal.

[39] Momma, K.; Izumi, F. (2011) *VESTA 3 for three-dimensional visualization of crystal, volumetric and morphology data*. Journal of Applied Crystallography 44, H. 6, S. 1272–1276. https://doi.org/10.1107/S0021889811038970

[40] Matschei, T.; Lothenbach, B.; Glasser, F. P. (2007) *The role of calcium carbonate in cement hydration.* Cement and Concrete Research 37, H. 4, S. 551–558.

[41] Matschei, T.; Lothenbach, B.; Glasser, F. P. (2007) *Thermodynamic properties of Portland cement hydrates in the system $CaO–Al_2O_3–SiO_2–CaSO_4–CaCO_3–H_2O$.* Cement and Concrete Research 37, H. 10, S. 1379–1410. https://doi.org/10.1016/j.cemconres.2007.06.002

[42] Georget, F. et al. (2022) *Stability of hemicarbonate under cement paste-like conditions*. Cement and Concrete Research 153, S. 106692. https://doi.org/10.1016/j.cemconres.2021.106692

[43] Damidot, D. et al. (1994) *Thermodynamic investigations of the $CaO{-}Al_2O_3{-}CaCO_3{-}H_2O$ closed system at 25°C and the influence of Na_2O*. Cement and Concrete Research 24, H. 3, S. 563–572.

[44] De Weerdt, K. et al. (2011) *Hydration mechanisms of ternary Portland cements containing limestone powder and fly ash*. Cement and Concrete Research 41, S. 279–291.

[45] De Weerdt, K. et al. (2010) *Fly ash-limestone ternary composite cements: synergetic effect at 28 days*. Nordic Concrete Research 42, H. 2, S. 51–70.

[46] De Weerdt, K. et al. (2011) *Synergy between fly ash and limestone powder in ternary cements.* Cement and Concrete Composites 33, H. 1, S. 30–38. https://doi.org/10.1016/j.cemconcomp.2010.09.006

[47] Antoni, M. et al. (2012) *Cement substitution by a combination of metakaolin and limestone*. Cement and Concrete Research 42, H. 12, S. 1579–1589. https://doi.org/10.1016/j.cemconres.2012.09.006

[48] Nied, D.; Stabler, C.; Zajac, M. (2015) *Assessing the synergistic effect of limestone and metakaolin*. Scrivener, K. L.; Favier, A. [Hrsg.] Proceeding of 1st International Conference on Calcined Clays for Sustainable Concrete. Lausanne, Switzerland, S. 245–251.

[49] Machner, A. et al. (2017) *Portland metakaolin cement containing dolomite or limestone – Similarities and differences in phase assemblage and compressive strength*. Construction and Building Materials 157, S. 214–225. https://doi.org/10.1016/j.conbuildmat.2017.09.056

[50] Hochstetter, C. (1842) *Untersuchung über die Zusammensetzung einiger Mineralien.* Journal für Praktische Chemie 27, S. 375–378.

[51] Allmann, R.; Jespen, H. P. (1969) *Die Struktur des Hydrotalkits*. Neues Jahrbuch für Mineralogie (Monatshefte) 12, S. 544–551.

[52] Zajac, M. et al. (2014) *Effect of $CaMg(CO_3)_2$ on hydrate assemblages and mechanical properties of hydrated cement pastes at 40 °C and 60 °C*. Cement and Concrete Research 65, S. 21–29.

[53] Ben Haha, M. et al. (2011) *Influence of slag chemistry on the hydration of alkali-activated blast-furnace slag – Part I: Effect of MgO*. Cement and Concrete Research 41, H. 9, S. 955–963. https://doi.org/10.1016/j.cemconres.2011.05.002

[54] Ben Haha, M. et al. (2012) *Influence of slag chemistry on the hydration of alkali-activated blast-furnace slag – Part II: Effect of Al_2O_3*. Cement and Concrete Research 42, H. 1, S. 74–83. https://doi.org/10.1016/j.cemconres.2011.08.005

[55] Morse, J. W.; Arvidson, R. S. (2002) *The dissolution kinetics of major sedimentary carbonate minerals*. Earth-Science Reviews 58, 1–2, S. 51–84. https://doi.org/10.1016/S0012-8252(01)00083-6

[56] Adu-Amankwah, S.; Black, L.; Zajac, M. (2015) *The effect of sulphates on limestone containing composite cements*. In: 35th Cement and Concrete Science Conference, University of Aberdeen.

[57] Koritnig, S.; Süsse, P. (1975) *Meixnerit, $Mg_6Al_2(OH)_{18}·4H_2O$, ein neues Magnesium-Aluminium-Hydroxid-Mineral*. Tschermaks mineralogische und petrographische Mitteilungen 22, S. 79–87.

[58] Arakcheeva, A. V. et al. (1996) *Crystal structure and comparative crystal chemistry of $Al_2Mg_4(OH)_{12}(CO_3)*3H_2O$, a new mineral from the hydrotalcite-manasseite group*. Crystallographic Reports 41, S. 972–981.

[59] Rössler, C.; Steiniger, F.; Ludwig, H. (2017) *Characterization of C-S-H and C-A-S-H phases by electron microscopy imaging, diffraction, and energy dispersive X-ray spectroscopy*. Journal of the American Ceramic Society 100, H. 4, S. 1733–1742. https://doi.org/10.1111/jace.14729

[60] Zajac, M.; Ben Haha, M. (2015) *Hydration of limestone and dolomite cement*. In: Proceedings of the 14th International Congress on the Chemistry of Cement, Beijing, China.

[61] Machner, A. et al. (2018) *Limitations of the hydrotalcite formation in Portland composite cement pastes containing dolomite and metakaolin.* Cement and Concrete Research 105, S. 1–17. https://doi.org/10.1016/j.cemconres.2017.11.007

[62] Machner, A. et al. (2018) *Stability of the hydrate phase assemblage in Portland composite cements containing dolomite and metakaolin after leaching, carbonation, and chloride exposure.* Cement and Concrete Composites 89, S. 89–106. https://doi.org/10.1016/j.cemconcomp.2018.02.013

[63] Balonis, M. et al. (2010) *Impact of chloride on the mineralogy of hydrated Portland cement systems.* Cement and Concrete Research 40, H. 7, S. 1009–1022. https://doi.org/10.1016/j.cemconres.2010.03.002

[64] Birnin-Yauri, U. A.; Glasser, F. P. (1998) *Friedel's salt, $Ca_2Al(OH)_6(Cl,OH)·2H_2O$: Its solid solutions and their role in chloride binding.* Cement and Concrete Research 28, H. 12, S. 1713–1723. https://doi.org/10.1016/S0008-8846(98)00162-8

[65] Glasser, F. P.; Kindness, A.; Stronach, S. A. (1999) *Stability and solubility relationships in AFm phases: Part I. Chloride, sulfate and hydroxide.* Cement and Concrete Research 29, S. 861–866. https://doi.org/10.1016/S0008-8846(99)00055-1

[66] Pöllmann, H. (1986) *Solid solutions of complex calcium aluminate hydrates containing Cl^-, OH^- and CO_3^{2-} - anions.* In: Proceedings of the 8th International Congress on the Chemistry of Cement. Rio de Janeiro, S. 300–306.

[67] Pöllmann, H. (1980) *Mischkristallbildung in den Systemen $3CaO·Al_2O_3·CaCl_2·10H_2O$ – $3CaO·Al_2O_3·CaCO_3·11H_2O$ und $3CaO·Al_2O_3·CaCl_2·10H_2O$ – $3CaO·Al_2O_3·Ca(OH)_2·12H_2O$ [Diploma Thesis].* Friedrich-Alexander-Universität Erlangen - Nürnberg.

[68] Hobbs, M. Y. (2001) *Solubilities and ion exchange properties of solid solutions between the OH, Cl and CO_3 end members of the monocalcium aluminate hydrates [PhD Thesis].* University of Waterloo.

[69] Wilson, W. et al. (2022) *Insights on chemical and physical chloride binding in blended cement pastes.* Cement and Concrete Research 156, S. 106747. https://doi.org/10.1016/j.cemconres.2022.106747

[70] Lothenbach, B. et al. (2019) *Cemdata18 – A chemical thermodynamic database for hydrated Portland cements and alkali-activated materials*. Cement and Concrete Research 115, S. 472–506. https://doi.org/10.1016/j.cemconres.2018.04.018

[71] De Weerdt, K. et al. (2015) *Impact of the associated cation on chloride binding of Portland cement paste*. Cement and Concrete Research 68, S. 196–202. https://doi.org/10.1016/j.cemconres.2014.01.027

[72] Arya, C.; Buenfeld, N. R.; Newman, J. B. (1990) *Factors influencing chloride-binding in concrete*. Cement and Concrete Research 20, H. 2, S. 291–300. https://doi.org/10.1016/0008-8846(90)90083-A

[73] Shi, Z. et al. (2017) *Role of calcium on chloride binding in hydrated Portland cement–metakaolin–limestone blends*. Cement and Concrete Research 95, S. 205–216. https://doi.org/10.1016/j.cemconres.2017.02.003

[74] Delagrave, A. et al. (1997) *Chloride Binding Capacity of Various Hydrated Cement Paste Systems*. Advanced Cement Based Materials 6, H. 1, S. 28–35. https://doi.org/10.1016/S1065-7355(97)90003-1

[75] Zhu, Q. et al. (2012) *Effect of chloride salt type on*

chloride binding behavior of concrete. Construction and Building Materials 37, S. 512–517. https://doi.org/10.1016/j.conbuildmat.2012.07.079

[76] Wowra, O.; Setzer, M. J. (1997) *Sorption of chlorides on hydrated cement and C_3S pastes*. Setzer, M. J.; Auberg, R. [Hrsg.] Frost Resistance of Concrete. London: E & FN Spon, S. 147–153.

[77] Tritthart, J. (1989) *Chloride binding in cement II. The influence of the hydroxide concentration in the pore solution of hardened cement paste on chloride binding*. Cement and Concrete Research 19, H. 5, S. 683–691. https://doi.org/10.1016/0008-8846(89)90039-2

[78] De Weerdt, K.; Orsáková, D.; Geiker, M. R. (2014) *The impact of sulphate and magnesium on chloride binding in Portland cement paste.* Cement and Concrete Research 65, S. 30–40. https://doi.org/10.1016/j.cemconres.2014.07.007

[79] Zibara, H. (2001) *Binding of external chlorides by cement pastes [PhD Thesis].* University of Toronto.

[80] Hemstad, P.; Machner, A.; De Weerdt, K. (2020) *The effect of artificial leaching with HCl on chloride binding in ordinary Portland cement paste.* Cement and Concrete Research 130, S. 105976. https://doi.org/10.1016/j.cemconres.2020.105976

[81] Machner, A. et al. (2022) *Effect of leaching on the composition of hydration phases during chloride exposure of mortar.* Cement and Concrete Research 153, S. 106691. https://doi.org/10.1016/j.cemconres.2021.106691

[82] Machner, A. et al. (2022) *Impact of leaching on chloride ingress profiles in concrete.* Materials and Structures 55, H. 1. https://doi.org/10.1617/s11527-021-01730-w

[83] Kuzel, H.-J. (1966) *Röntgenuntersuchung in System $3CaO{\cdot}Al_2O_3{\cdot}CaSO_4{\cdot}nH_2O–3CaO{\cdot}Al_2O_3{\cdot}CaCl_2{\cdot}nH_2O–H_2O$.* In: Neues Jahrbuch für Mineralogie (Monatshefte), S. 193–200.

[84] Lothenbach, B.; Durdziński, P. T.; De Weerdt, K. (2016) *Thermogravimetric Analysis.* In: Scrivener, K. L.; Snellings, R.; Lothenbach, B. [Hrsg.] A Practical Guide to Microstructural Analysis of Cementitious Materials. Boca Raton: CRC Press Taylor & Francis Group, S. 177–211.

[85] Shi, Z. et al. (2017) *Friedel's salt profiles from thermogravimetric analysis and thermodynamic modelling of Portland cement-based mortars exposed to sodium chloride solution.* Cement and Concrete Composites 78, S. 73–83. https://doi.org/10.1016/j.cemconcomp.2017.01.002

[86] Machner, A. et al. (2018) *Chloride-binding capacity of hydrotalcite in cement pastes containing dolomite and metakaolin.* Cement and Concrete Research 107, S. 163–181. https://doi.org/10.1016/j.cemconres.2018.02.002

[87] Thomas, M.D.A. et al. (2012) *The effect of supplementary cementitious materials on chloride binding in hardened cement paste.* Cement and Concrete Research 42, H. 1, S. 1–7. https://doi.org/10.1016/j.cemconres.2011.01.001

[88] Witzke, T. et al. (2012) *Use of Layered Double Hydroxides (LDH) of the Hydrotalcite Group as Reservoir Minerals for Nitrate in Soils – Examination of the Chemical and Mechanical Stability.* In: Krivovichev, S. V. [Hrsg.] Minerals as Advanced Materials II. Berlin, Heidelberg: Springer Berlin Heidelberg, S. 131–145.

[89] de Roy, A. (1998) *Lamellar Double Hydroxides in: Molecular Crystals and Liquid Crystals Science and Technology.* Section A. Molecular Crystals and Liquid Crystals 311, H. 1, S. 173–193. https://doi.org/10.1080/10587259808042384

[90] De Weerdt, K. et al. (2016) *Towards the understanding of chloride profiles in marine exposed concrete, impact of leaching and moisture content.* Construction and Building Materials 120, S. 418–431. https://doi.org/10.1016/j.conbuildmat.2016.05.069

[91] Ye, H. et al. (2016) *Prediction of chloride binding isotherms for blended cements.* Computers and Concrete 17, H. 5, S. 655–672. https://doi.org/10.12989/cac.2016.17.5.655